Redox Biology 57 (2022) 102475

Contents lists available at ScienceDirect

Redox Biology

journal homepage: www.elsevier.com/locate/redox

Mitochondrial ferritin alleviates apoptosis by enhancing mitochondrial bioenergetics and stimulating glucose metabolism in cerebral ischemia reperfusion

Peina Wang [a,b], Yanmei Cui [a], Yuanyuan Liu [a], Zhongda Li [a], Huiyuan Bai [a], Yashuo Zhao [a,c], Yan-Zhong Chang [a,*]

[a] Laboratory of Molecular Iron Metabolism, Key Laboratory of Animal Physiology, Biochemistry and Molecular Biology of Hebei Province, College of Life Science, Hebei Normal University, Shijiazhuang, 050024, Hebei Province, China
[b] College of Basic Medicine, Hebei Medical University, Shijiazhuang, 050017, Hebei Province, China
[c] Scientific Research Center, Hebei University of Chinese Medicine, Shijiazhuang, 050200, Hebei Province, China

ARTICLE INFO

Keywords:
Mitochondrial ferritin
Ischemic stroke
Mitochondrial bioenergetics
Glucose metabolism
G6PDH

ABSTRACT

Oxidative stress and deficient bioenergetics are key players in the pathological process of cerebral ischemia reperfusion injury (I/R). As a mitochondrial iron storage protein, mitochondrial ferritin (FtMt) plays a pivotal role in protecting neuronal cells from oxidative damage under stress conditions. However, the effects of FtMt in mitochondrial function and activation of apoptosis under cerebral I/R are barely understood. In the present study, we found that FtMt deficiency exacerbates neuronal apoptosis via classical mitochondria-depedent pathway and the endoplasmic reticulum (ER) stress pathway in brains exposed to I/R. Conversely, FtMt overexpression significantly inhibited oxygen and glucose deprivation and reperfusion (OGD/R)-induced apoptosis and the activation of ER stress response. Meanwhile, FtMt overexpression rescued OGD/R-induced mitochondrial iron overload, mitochondrial dysfunction, the generation of reactive oxygen species (ROS) and increased neuronal GSH content. Using the Seahorse and O2K cellular respiration analyser, we demonstrated that FtMt remarkably improved the ATP content and the spare respiratory capacity under I/R conditions. Importantly, we found that glucose consumption was augmented in FtMt overexpressing cells after OGD/R insult; overexpression of FtMt facilitated the activation of glucose 6-phosphate dehydrogenase and the production of NADPH in cells after OGD/R, indicating that the pentose-phosphate pathway is enhanced in FtMt overexpressing cells, thus strengthening the antioxidant capacity of neuronal cells. In summary, our results reveal that FtMt protects against I/R-induced apoptosis through enhancing mitochondrial bioenergetics and regulating glucose metabolism via the pentose-phosphate pathway, thus preventing ROS overproduction, and preserving energy metabolism.

1. Introduction

Stroke affects 13.7 million people globally per year and is the second leading cause of death worldwide [1]. Most strokes are ischemic due to vascular occlusion, resulting from multiple events, such as large artery atherosclerosis, cardiac diseases and small vessel disease [2]. Despite a large number of clinical studies, most novel treatment strategies have failed to translate to clinic; thrombolysis, with tissue-type plasminogen activator or endovascular devices, remains the only available treatment [3]. While thrombolysis treatment restores the blood flow to the ischemic brain, the rapid reperfusion itself can cause secondary injury, referred to as ischemia/reperfusion injury (I/R), by promoting free radical accumulation, inflammatory response and the degradation of the blood-brain barrier [4]. Therefore, I/R injury is an inevitable problem under the current treatment options for ischemic stroke; it is critical to identify additional neuroprotective approaches that can be used to mitigate I/R injury.

Increased generation of reactive oxygen species (ROS) has been identified as a major reason to the pathological mechanisms underlying cerebral I/R injury [5], and the mitochondrial respiratory chain has

* Corresponding author. Laboratory of Molecular Iron Metabolism, College of Life Science, Hebei Normal University, 20, Nanerhuan Eastern Road, Shijiazhuang, 050024, Hebei Province, China.
E-mail addresses: yzchang@hebtu.edu.cn, chang7676@163.com (Y.-Z. Chang).

https://doi.org/10.1016/j.redox.2022.102475
Received 5 September 2022; Accepted 11 September 2022
Available online 24 September 2022

been shown to be the main source of ROS after I/R [6,7]. Impaired mitochondrial oxidative metabolism and a depletion of energy of neuronal cells during ischemia contribute to the initiation of apoptosis [8]. Following ischemia, severe oxygen and glucose deprivation induces mitochondrial dysfunction, leading to a disruption in energy metabolism and an overproduction of ROS [9]. After reperfusion, mitochondria use oxygen as a substrate to generate ROS [10]. The excessive ROS may induce the opening of the mitochondrial transition pore and depolarizing the mitochondrial membrane, subsequently leading to the release of pro-apoptotic factors and activation of the mitochondria-dependent apoptosis pathway in the brain [11,12]. In addition, recent studies have implicated that the increased ROS can also initiate endoplasmic reticulum (ER) stress-mediated apoptosis in the pathological processes of I/R injury [13]. The ER is an integral cellular component that mediates both the maturation of newly synthesized proteins and intracellular calcium homeostasis [14]. Cerebral I/R-induced inflammation, calcium dysregulation and accumulation of ROS can perturb ER function, resulting in an accumulation of unfolded and misfolded proteins in the ER lumen, which subsequently triggers the unfolded protein response (UPR), leading to ER stress [15]. At early stages, the UPR is a protective response aimed at restoring ER function, however, if the stress is severe or prolonged, the UPR can result in apoptosis. Therefore, oxidative damage and mitochondrial dysfunction are consequences of cerebral I/R; this damage, in turn, further facilitates ROS production and leads to activation of the mitochondria-dependent and ER stress-mediated apoptosis.

Mitochondrial ferritin (FtMt) is a mitochondrial iron storage protein that possesses ferroxidase activity, which permits the storage of ferric iron, as opposed to the reactive, ferrous form of the metal [16]. FtMt is highly expressed in tissues characterized by high metabolic activity and oxygen consumption, such as the brain, testes and heart, but not in liver and spleen, which exsert main iron storage function for the body and express high levels of cytosolic ferritins [17]. Since the mitochondria, which generate both heme and iron-sulfur clusters, are exposed to heavy iron traffic and excessive free iron facilitates the generation of toxic ROS via the Fenton reaction, the function of FtMt inside mitochondria is likely to protect mitochondria from oxidative damage, rather than to act an iron storage protein for cellular and/or systemic needs [18]. Increasing evidence has indicated that FtMt is an important antioxidant component under stress conditions. FtMt has been shown to reverse neuronal apoptosis and oxidative stress in mouse models of Alzheimer's and Parkinson's disease and to protect SH-SY5Y cells from H_2O_2-induced oxidative stress by inhibiting free iron accumulation [19–22]. In addition, a previous study has shown that FtMt rescues frataxin deficiency-induced impairment of respiratory function, indicating that FtMt may be involved in maintaining mitochondrial bioenergetics and cell metabolism [23]. Our recent study indicated that FtMt was upregulated in the brain of I/R and FtMt deficiency aggravated I/R-induced iron overload and the activation of ferroptosis [24]. In addition, we have also observed increased numbers of ruptured mitochondria in brains of FtMt deficient mice compared with wild-type mice after I/R. However, the effects of FtMt on cerebral I/R-induced mitochondrial dysfunction and apoptosis have not been investigated.

In the present study, we used *Ftmt*-knockout mice and a FtMt-overexpressing cell line as well as mouse models of middle cerebral artery occlusion (MCAO) stroke and oxygen-glucose deprivation followed by reoxygenation (OGD/R). We found that FtMt alleviates mitochondria-dependent apoptosis and ER stress pathway (ATF4/ATF6-CHOP)-mediated apoptosis under I/R by inhibiting mitochondrial dysfunction and mitochondrial ROS accumulation. Mechanically, our results provide novel insight into the neuroprotective and antioxidative properties of FtMt, which enhances mitochondrial bioenergetics and stimulates glucose metabolism via the pentose-phosphate pathway, thus inhibiting ROS generation and preserving energy homeostasis in neurons during I/R injury.

2. Materials and methods

2.1. Mice

Three-month-old C57BL/6 J wild-type male mice and *Ftmt*-knockout male mice were used in this study. The wild-type mice and *Ftmt*-knockout mice were originally generated by Dr. M. Fleming's group [25]; we obtained the mice from The Jackson Laboratory. The mice were genotyped by PCR amplification of genomic DNA (Supplementary Fig. 1A), and FtMt expression in brain of mice were verified by qPCR from total RNA (Supplementary Fig. 1B; primer sequences provided in Supplementary Table 1), Western blot analysis of FtMt protein expression in the brain (Supplementary Fig. 1C) and the distribution of FtMt in wild-type and FtMt-knockout mouse neurons by double immunofluorescence (Supplementary Fig. 1E). All animals were housed in an environment with controlled temperature (22–24 °C), standard lighting conditions (12 h light/dark cycle) and humidity (45–55%) and with free access to food and water. The investigators were blinded to the randomly assigned genotypes and samples for all experiments until after the analysis was completed. All procedures were carried out in accordance with the National Institutes of Health Guide for the Care and Use of Laboratory Animals and were approved by the Animal Care and Use Committee of the Hebei Science and Technical Bureau in China.

2.2. Middle cerebral artery occlusion (MCAO)

Focal ischemia was induced via MCAO in mice, as described previously [26,27]. Briefly, the mice were anaesthetized with an intraperitoneal injection of chloral hydrate (3.5 mg/kg), and the body temperature was maintained at 37 °C with a warming blanket. After making a midline incision in the neck, the common carotid artery (CCA), external carotid artery (ECA) and internal carotid artery (ICA) were exposed. Next, a nylon monofilament (602234 PK, Doccol Corp, CA, USA) was delivered to the ICA through the ECA stump. Cerebral blood flow was monitored by laser Doppler flowmetry (Perimed, Sweden). A blood flow drop of >75% below the baseline was considered successfully occluded. After an occlusion period of 90 min, the suture was gently removed to initiate reperfusion. The mice were allowed free access to water and food after the surgery.

2.3. Cell culture and OGD/R model

The stable FtMt-overexpressing SH-SY5Y cell line (FtMt-SY5Y), a pcDNA3.1 (−) empty vector-transfected cell line (Vector-SY5Y) and wild-type SH-SY5Y (WT-SY5Y) cell line were generated as described previously [28]. We confirmed the overexpression of FtMt in the FtMt-SY5Y cell line by Western blot analysis (Supplementary Fig. 1D). The cells were cultured in Dulbecco's modified Eagle's medium (DMEM; Gibco, CA, USA) supplemented with 10% fetal bovine serum (Gibco) and 1% penicillin-streptomycin (#10378016, Sigma-Aldrich, USA) in a 37 °C humidified incubator with 5% CO_2. Briefly, the three types of cells were cultured under normal conditions for 24 h, then the cells were washed twice in glucose-free DMEM (Gibco) and transferred to this medium. Cells were placed in a hypoxic chamber with 1% O_2, 5% CO_2 and 94% N_2 at 37 °C for 5 h. Finally, the medium was discarded and the cells were cultured for an additional 18 h for reperfusion in normoxic, glucose-containing medium under normal conditions.

2.4. Assessment of apoptosis by flow cytometry and TUNEL staining

After 24 h reperfusion, the mice were anaesthetized and then fixed by transcardial perfusion with saline followed by 4% paraformaldehyde. The brains were immediately removed and postfixed in 4% paraformaldehyde for 4 h and then cut into 15 μm sections. Terminal deoxynucleotidyl transferase (TdT)-mediated dUTP nick-end labeling (TUNEL) *In Situ* Cell Death Detection Kit (#12156792910, Roche,

Mannheim, Germany) was performed to evaluate apoptosis in the brain and the procedures were carried out following the manufacturer's instructions. Briefly, the brain sections were washed twice with phosphate buffer solution (PBS) and incubated with 50 μL TUNEL reaction mixture for 60 min at 37 °C in the dark. Next, the sections were washed three times with PBS and incubated with 4′,6-iamidino-2-phenylindole (DAPI) for 4 min. The images were captured with an Olympus FV3000 confocal laser scanning microscope. The data are presented as the percentage of the number of TUNEL-positive cells in five randomly-selected fields.

Apoptosis after OGD/R treatment was detected with a FITC-Annexin V apoptosis detection kit (#C1062L, Beyotime, Shanghai, China) according to the manufacturer's instructions. After OGD/R treatment, the cells were harvested and stained with annexin-V for 10 min at 37 °C. The cells were then centrifuged at 1000×*g* for 5 min at room temperature. After washing twice with PBS, the cells were stained with propidium iodide (PI). The percentage of apoptotic cells was analyzed by flow cytometry (CytoFLEX, Beckman Coulter).

2.5. ROS assessment

In vivo ROS production in brain sections of mice after I/R injury was analyzed using dihydroethidium (DHE, #37291, Sigma-Aldrich, USA) staining, as previously reported [29]. The sections were washed twice with PBS and then incubated with 5 μM DHE for 30 min at 37 °C. After washing three times with PBS, the nuclei were stained with DAPI. The fluorescence intensity of the DHE-positive cells was quantified by ImageJ software.

2.6. Mitochondrial membrane potential (MMP) assessment

The MMP in cells treated by OGD/R was determined using JC-1, a cationic dye of 5,5′,6,6′-tetrachlorol, 1′,3,3′-tetraethyl benzimidazole (#T3168, Invitrogen, USA), according to the manufacturer's instructions. After OGD/R treatment, the cells were washed twice with PBS and incubated with 10 μg/mL JC-1 at 37 °C for 30 min. Images were captured using a fluorescence microscope (Leica, Germany).

2.7. Mitochondrial ROS detection

The production of mitochondrial ROS in cells after OGD/R insult was assessed with the MitoSOX red mitochondrial superoxide indicator (#M36008, Invitrogen, USA). The cells were harvested and washed twice with Hanks balanced salt solution (HBSS). The cells were then incubated in 500 μL of HBSS containing 5 μM MitoSOX for 10 min at 37 °C in the incubator (5% CO_2). After washing three times in HBSS, the cells were analyzed by flow cytometry or confocal microscopy.

2.8. Detection of intracellular ATP content

The ATP content of cells after OGD/R treatment was evaluated using an ATP assay kit (#S0026, Beyotime, Shanghai, China) according to the manufacturer's instructions. In brief, the cells were lysed and centrifuged at 12000×*g* for 5 min. Next, 100 μL supernatant was removed into a 96-well plate and mixed with 100 μL ATP working solution for 5 min at room temperature. The ATP levels in each group was measured using a microplate reader. For detailed instructions, see supplementary document 1.

2.9. Measurement of glutathione (GSH) and malondialdehyde (MDA)

The GSH and MDA content was measured in WT-SY5Y, Vector-SY5Y, and FtMt-SY5Y cell lines after OGD/R treatment using commercial kits (#S0053, #S0131M, Beyotime, Shanghai, China). The evaluation was carried out according to the protocol provided by the manufacturer. For GSH assessment, cells were washed with PBS and then centrifuged to collect the cells. First, the protein removal reagent solution was added to the cells and two rapid freeze-thaw cycles were performed on the samples. Afterwards, the samples were centrifuged at 10000×*g* for 10 min. The supernatant was mixed with the GSH assay regent and incubated at 25 °C for 5 min. Finally, the absorbance at 412 nm was measured using a microplate reader. The GSH content of each group was calculated based on a the standard curve. The MDA content was assessed using the thiobarbituric acid (TBA) method, which is based on spectrophotometric measurement of the product of the reaction of TBA with MDA. The MDA concentrations were calculated by the absorbance of the product at 532 nm. For detailed instructions, see supplementary document 1.

2.10. Measurement of NADPH content

The NADPH content of cells after OGD/R treatment was evaluated using an NADPH assay kit (#S0179, Beyotime, Shanghai, China) according to the manufacturer's instructions. Briefly, the cells were treated with extraction solution and centrifuged at 10000×*g* for 10 min. Then the supernatant was incubated at 60 °C for 30 min to decompose the $NADP^+$. After cooling on ice, the supernatant was reacted with a working solution for 20 min at 37 °C and the absorbance was measured at 450 nm. For detailed instructions, see supplementary document 1.

2.11. Determination of glucose-6-phosphate dehydrogenase (G6PDH) activity

G6PDH activity was measured using a commercial kit (#S0189, Beyotime, Shanghai, China). The procedures were carried out according to the manufacturer's instructions. Briefly, the cells were treated with extraction solution and centrifuged at 12000×*g* for 10 min. Next, 50 μL supernatant was removed into a 96-well plate and incubated with 50 μL G6PDH working solution for 10 min at room temperature in the dark. The absorbance was measured at 450 nm. For detailed instructions, see supplementary document 1.

2.12. Mitochondrial ferrous iron staining

To evaluate mitochondrial iron content, cells were incubated with Mito-Ferro Green (#M489, Dojindo) according to the manufacturer's instructions. In brief, the cells were washed twice with HBSS and then incubated with 5 μM Mito-Ferro Green in HBSS for 30 min at 37 °C. The nuclei were counterstained with Hoechst. After washing three times with PBS, the fluorescence was observed using a fluorescence microscope. The fluorescence intensity was quantified by ImageJ software.

2.13. Western blot analysis

Protein expression was detected by Western blot analysis as previously described [30]. The following antibodies were used: anti-β-actin (1:10000) was obtained from Sigma-Aldrich (#A5441, St. Louis, MO, USA); anti-GRP78 (1:5000), anti-phosphorylated EIF2α (1: 2000), anti-EIF2α (1:2000), anti-XBP1 (1:5000), anti-caspase12 (1:5000) and anti-ATF4 (1:2000) were obtained from Abcam Trading [Shanghai] Company Ltd. (#ab21685, #ab32157, #ab169528, #ab37152, #ab62463, #ab1371, respectively); anti-ATF6 (1:3000) was obtained from ABclonal Biotechnology, Boston, USA (#A2570); anti-P-Erk1/2 (1:2000), anti-Erk1/2 (1:2000), anti-caspase3 (1:5000), anti-Bcl-2 (1:2000) and anti-Bax (1:2000) were obtained from Cell Signaling Technology, Danvers, MA, USA (#4370, #4695, #14220, #3498, #2772, respectively); anti-CHOP (1:1000) was obtained from GeneTex, Irvine, USA (#GTX32616); anti-Mfrn1 (1:2000) was obtained from Proteintech, Wuhan, China (#26469-1-AP). The immunoreactive proteins were detected using the enhanced chemiluminescence (ECL) method and quantified by transmittance densitometry using ImageJ software.

2.14. Measurement of mitochondrial bioenergetics and glucose metabolism

Mitochondrial oxygen consumption rate (OCR) and extracellular acidification rate (ECAR) of cells after OGD/R treatment were measured using a Seahorse XFp Analyzer. The Seahorse XF cell mito stress test kit (#103010-100) and Seahorse XF glycolysis stress test kit (#103017-100) were used as per the manufacturer's instructions. Briefly, the cells were plated on Seahorse XFp microplates at a concentration of 1×10^4 cells/well. After OGD/R treatment, the cells were washed twice with assay medium (#103575-100, Seahorse Bioscience) and incubated in a non-CO_2 incubator at 37 °C for 45 min. The microplates were then loaded into the analyzer and three compounds, oligomycin (2 μM), carbonylcyanide-4-(trifluoromethoxy) phenylhydrazone (FCCP, 8 μM) and a mixture of antimycin and rotenone (1 μM) were sequentially injected into the samples during the OCR measurement. ECAR was recorded after the sequential injections of glucose (10 mM), oligomycin (2 μM) and 2-deoxyglucose (2-DG, 50 mM). The OCR and ECAR values in each well were normalized to the well's protein concentration.

Mitochondrial function of cells in the brain of mice after cerebral I/R was analyzed using an Oxygraph-2k (O2k) system (Oroboros, Innsbruck, Austria), as reported previously [31]. Briefly, 10 mg brain tissue was immersed in 2 mL pre-chilled MIR05 buffer and the tissue was homogenized using a homogenizer. The supernatant was used to detect mitochondrial respiration following a substrate-uncoupler-inhibitor titration (SUIT, #D034) protocol. OCR values were recorded with sequential injections of 5 mM pyruvate, 2 mM malate, 2.5 mM ADP, 1 μM oligomycin, 4 μM FCCP and a mixture of antimycin and rotenone (1 μM).

2.15. Statistical analysis

Statistical analysis was performed using GraphPad Prism-6 and SPSS 16.0. All data are presented as the mean ± SEM. Comparisons between two groups were made using Student's t-test (two-tailed). One-way ANOVA with Tukey's post hoc test was used for multi-group comparisons. A value of $p < 0.05$ was considered statistically significant.

3. Results

3.1. FtMt ablation aggravates cerebral I/R-induced apoptosis

To explore whether FtMt affords protective effects against neuronal apoptosis under ischemic stroke, we performed MCAO surgery on wild-type (WT) and *Ftmt*-knockout (KO) mice, to establish a cerebral I/R mouse model, and quantified apoptotic cells in the uninjured hemisphere (Con group) and I/R-injured hemisphere (I/R group) by TUNEL staining. The number of TUNEL-positive cells in the ischemic cortex of KO mice was markedly greater than that in WT mice after I/R injury (Fig. 1A). We further detected the expression of markers of mitochondria-mediated apoptosis in WT and KO mice after I/R. As shown in Fig. 1B, the Bcl-2/Bax ratio was decreased, whereas the activation of cleaved caspase-3 (Fig. 1C) was significantly increased, in the *Ftmt* KO I/R group, compared with the WT I/R group. In addition, previous studies have demonstrated that increased reactive oxygen species and excessive excitation of glutamate receptors in the brain after ischemia reperfusion can result in significant increases in the phosphorylation of ERK1/2 [32–36]. We observed significantly increased

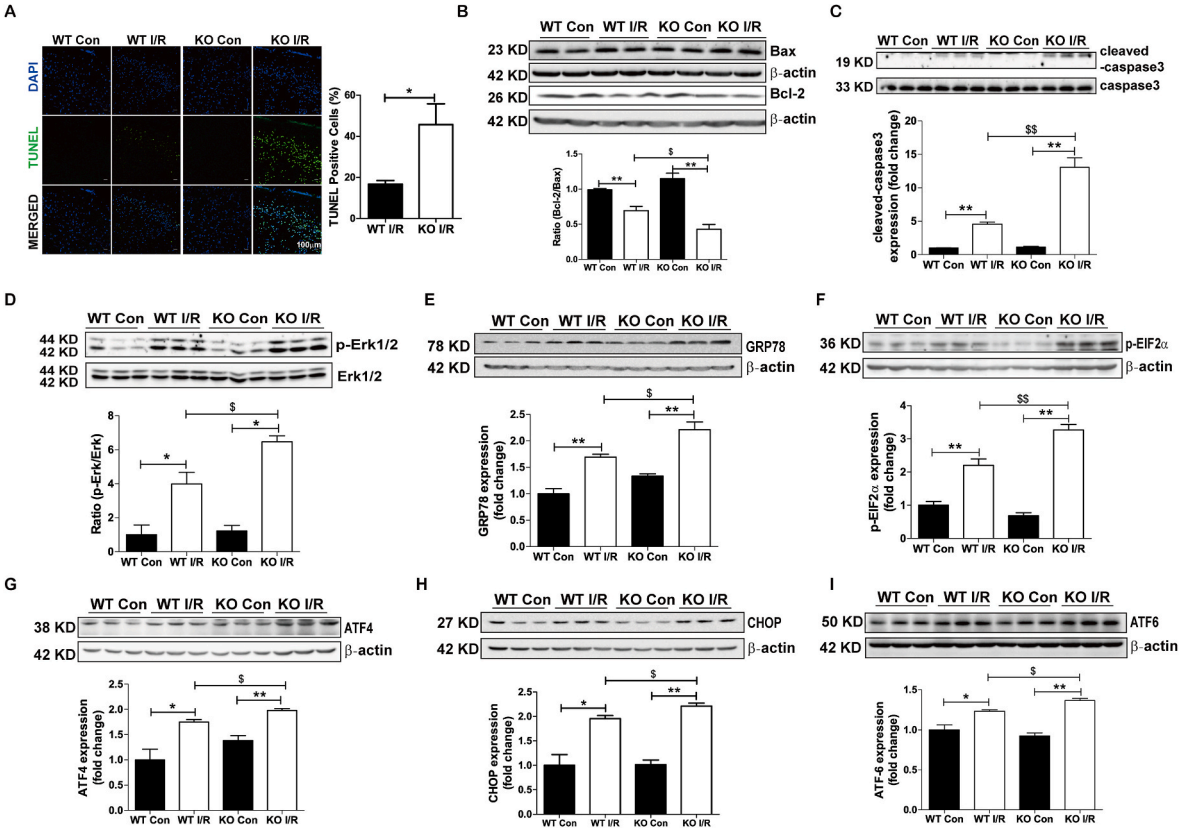

Fig. 1. FtMt ablation aggravates cerebral I/R-induced apoptosis. Apoptotic cell death was assessed by DAPI and TUNEL staining. (A) Representative photographs of uninjured and injured cortices of the mouse brains (left panels). The DAPI-stained, TUNEL-positive cells were counted (right panel). (B–I) Western blot and densitometric analyses of (B) the ratio of Bcl-2 to Bax, (C) the amount of cleaved caspase 3, and (D) the ratio of p-Erk1/2 to Erk1/2, (E) GRP78, (F) p-EIF2α, (G) ATF4, (H) CHOP, and (I) ATF6 in wild-type (WT) and *Ftmt*-knockout (KO) mice after MCAO (90 min) and subsequent reperfusion (24 h). I/R, penumbral area in the cortex of the injured hemisphere; Con, corresponding area in the cortex of the uninjured hemisphere. The results are presented as the mean ± SEM. n = 3, $^{*/\$}P < 0.05$, $^{**/\$}{}^{\$}P < 0.01$.

p-Erk1/2 in the KO I/R group than in the WT I/R group (Fig. 1D). Although Erk1/2 activation has also been reported to be pro-survival effect in ischemic stroke [37], we propose that phenomenon may be related to differences in timing of the ischemia and reperfusion, as well as the region of I/R brain we detected. Thus, the deletion of FtMt exacerbated mitochondria-dependent apoptosis under I/R.

Previous studies have shown that overproduction of ROS can initiate the ER stress response, ultimately resulting in neuronal apoptosis in I/R injury [38]. In order to assess whether the increased apoptosis in *Ftmt*-knockout mice is also related to the activation of ER stress pathways, we examined the expression of ER stress markers in mice after I/R injury. There are three main pathways involved in ER stress: the XBP1 (X-box-binding protein 1) pathway, the EIF2α (eukaryotic initiation factor 2 alpha)-ATF4 (activating transcription factor-4) pathway and the ATF6 pathway. As shown in Fig. 1E, the expression of GRP78 (glucose-regulated protein 78), a major marker of ER stress, was increased in the *Ftmt* KO I/R group, indicating that the deletion of FtMt exacerbated the I/R-induced ER stress response. Next, we observed a greater activation of EIF2α and upregulation of ATF4, CHOP and ATF6 in *Ftmt*-knockout mice than in WT mice after I/R injury, which implies that the ablation of *Ftmt* promoted the activation of the EIF2α and ATF6 pathways (Fig. 1F–I). In addition, the levels of XBP1 and caspase 12 did not change in our model (Supplementary Figs. 2A–B). Together, these results suggest that FtMt deficiency aggravates both mitochondria-dependent and ER stress-mediated apoptosis in cerebral I/R.

3.2. Overexpression of FtMt alleviates OGD/R injury-induced apoptosis

Oxygen-glucose deprivation-reoxygenation (OGD/R) is a widely accepted model for studying ischemic reperfusion *in vitro* [39,40]. To further verify the anti-apoptosis role of FtMt in I/R, we measured apoptosis in SH-SY5Y cells (WT group), stable FtMt-overexpressing SH-SY5Y cells (FtMt group) and pcDNA3.1 (−) empty vector-transfected cells (Vector group) after OGD/R insult. FtMt overexpression markedly decreased OGD/R-induced apoptosis. As shown in Fig. 2A, the percentage of apoptotic cells rose to nearly 25% after OGD/R insult in WT and Vector cells, while it was significantly decreased in the FtMt OGD/R group. Consistent with the *in vivo* data, we found that the increased expression of GRP78 and activation of the EIF2α-ATF4/ATF6 pathway induced by OGD/R were notably diminished by FtMt overexpression (Fig. 2B–E). Therefore, these results confirm that FtMt overexpression inhibits OGD/R-induced apoptosis.

3.3. FtMt deletion promotes ROS generation and decreases mitochondrial bioenergetics during cerebral I/R

Previous studies have shown that increased levels of ROS are responsible for the increased apoptosis in cerebral I/R. Our recent results indicate that FtMt deficiency promotes lipid peroxidation in I/R brains [24]. In the present study, we further evaluated ROS generation in the uninjured and I/R-injured hemispheres of WT and KO mice by DHE staining. The fluorescence was significantly increased in the I/R injured hemisphere, with the ROS generation increase more pronounced in KO mice compared to WT mice (Fig. 3A–B), indicating that FtMt deficiency aggravates I/R-induced oxidative stress. Cerebral I/R causes mitochondrial damage, with the impaired mitochondria promoting the generation of ROS in neuronal cells [41]. To examine the effects of FtMt on mitochondrial bioenergetics during cerebral I/R, we measured mitochondrial oxygen consumption rate (OCR) in wild-type and *Ftmt*-knockout mice using an O2k Analyzer. As shown in Fig. 3C, the basal respiration of neuronal cells from I/R-injured cortex was significantly decreased compared with the control; the deletion of FtMt exacerbated this decline. The first compound added in the analysis workflow, oligomycin, a complex V inhibitor, was injected to evaluate ATP-linked respiration. Next, FCCP, a mitochondrial uncoupler, was injected to determine the maximal respiration and the spare respiratory capacity. Finally, a mixture of rotenone (inhibitor of complex I) and antimycin A (inhibitor of complex III) were added to assess non-mitochondrial respiration. After I/R injury, the ATP production-linked oxygen consumption rate (Fig. 3D), the maximal respiration (Fig. 3E) and the spare respiratory capacity (Fig. 3F) were

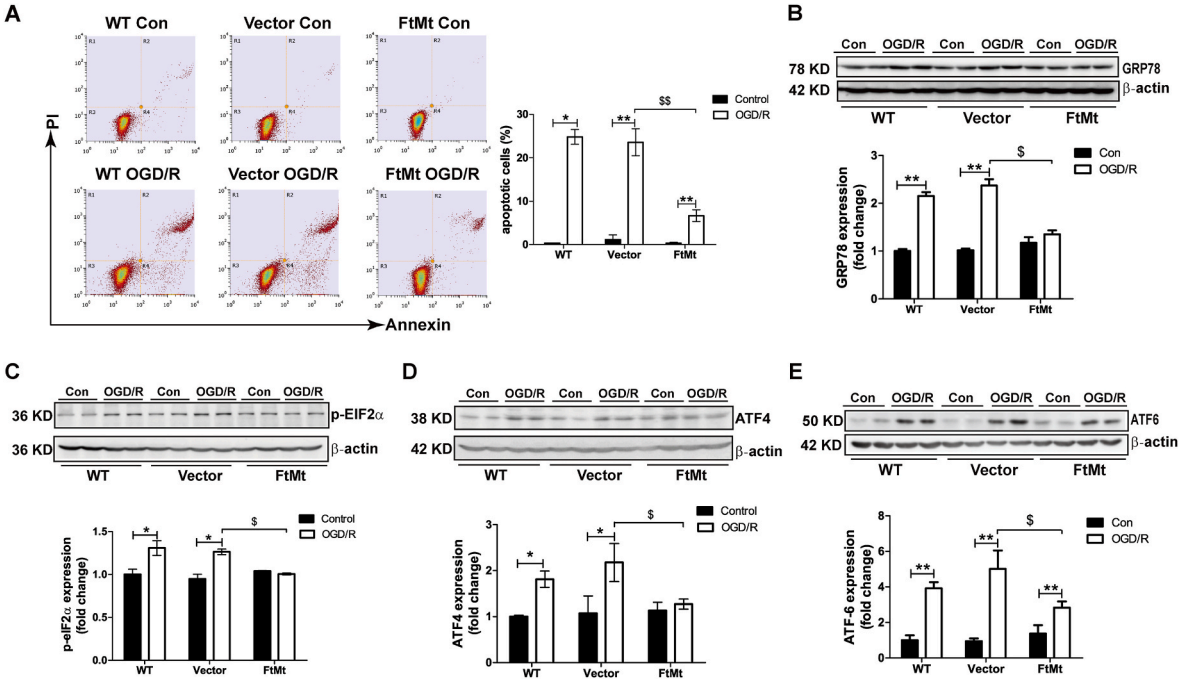

Fig. 2. Overexpression of FtMt decreases OGD/R injury-induced apoptosis. SH-SY5Y cells (WT), stable FtMt-overexpressing SH-SY5Y cells (FtMt) and pcDNA3.1 (−) empty vector-transfected cells (Vector) were subjected to OGD/R insult. (A) Apoptosis, as measured by flow cytometry. The right panel shows the proportion of apoptotic cells in the different groups. The levels of (B) GRP78, (C) p-EIF2α, (D) ATF4, and (E) ATF6, as assessed by Western blot (n = 4). The results are presented as the mean ± SEM. $^{*/\$}P < 0.05$, $^{**/\$\$}P < 0.01$.

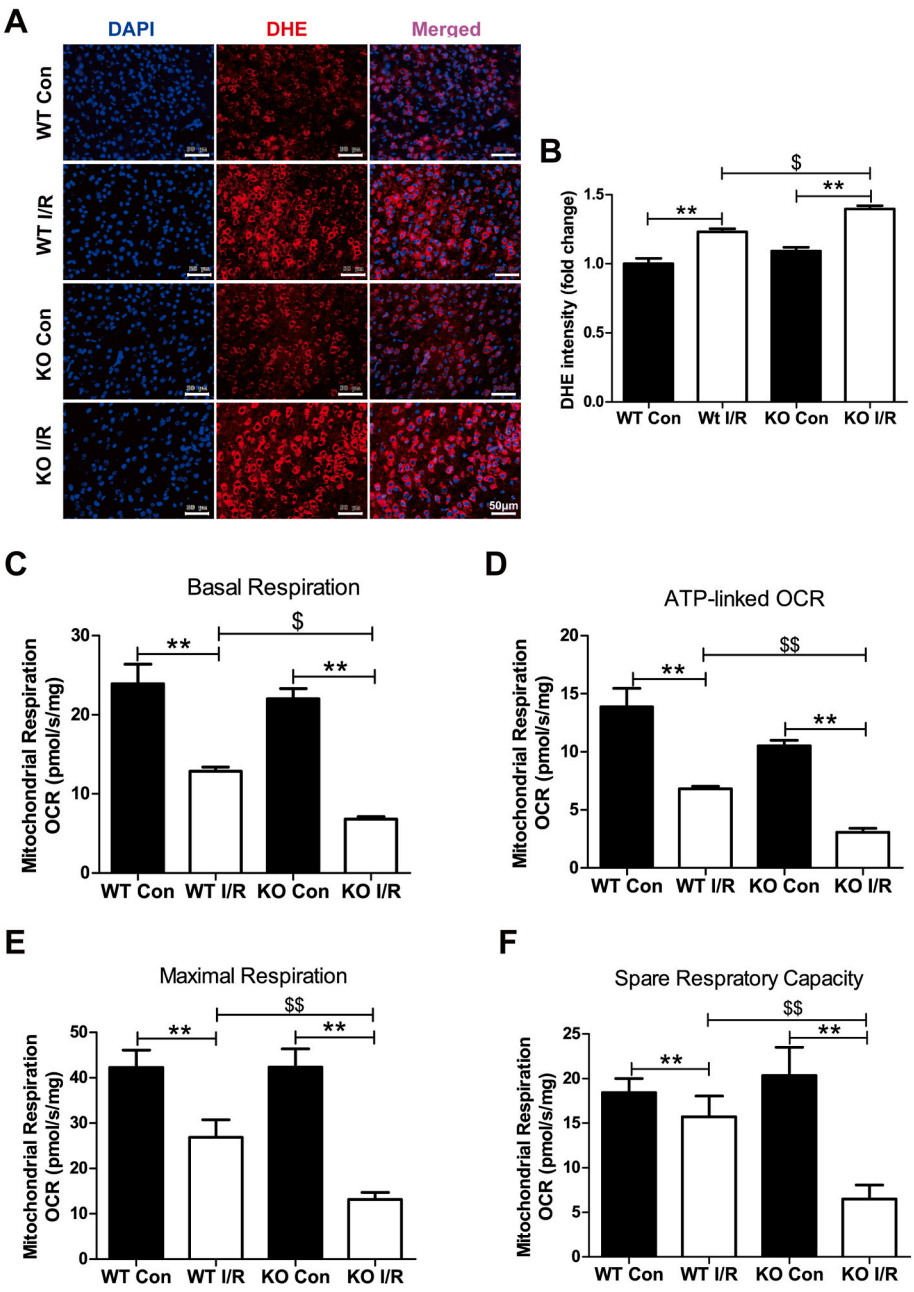

Fig. 3. FtMt deletion promotes ROS generation and decreases mitochondrial bioenergetics during cerebral I/R. (A) ROS generation in brain slices from wild-type mice and *Ftmt*-knockout mice after I/R treatment (MCAO, 90 min followed by 24 h reperfusion), as determined by dihydroethidium (DHE) staining. (B) Quantitative evaluation of DHE fluorescence intensity (n = 3). Wild-type and *Ftmt*-knockout mice were subjected to I/R. Next, the oxygen consumption rate (OCR) of the Con and I/R groups was determined using an O2K analyzer. OCR was recorded at baseline and after the sequential injection of oligomycin (1 μM), FCCP (4 μM) and a mixture of rotenone and antimycin A (1 μM). (C) Basal respiration, (D) ATP -linked OCR, (E) maximal respiration and (F) spare respiratory capacity were calculated (n = 4). The results are presented as the mean ± SEM. $^{\$}P < 0.05$, $^{**/\$\$}P < 0.01$.

remarkably diminished in the WT I/R and KO I/R groups, compared with the control. These decreases were significantly enhanced in *Ftmt*-knockout neuronal cells. Thus, FtMt plays an important role in maintaining mitochondrial bioenergetics and preventing ROS generation during cerebral I/R.

3.4. *FtMt overexpression restricts ROS generation and enhances mitochondrial bioenergetics during OGD/R injury*

To further verify the role of FtMt we observed *in vivo*, we explored the effects of FtMt on ROS regulation and mitochondrial bioenergetics using a FtMt-overexpressing cell line in the OGD/R model. Since mitochondria, particularly damaged mitochondria, are the main source of ROS, we measured mitochondrial ROS generation in SH-SY5Y cells (WT group), pcDNA3.1 (−) empty vector-transfected cells (Vector group) and stable FtMt-overexpressing SH-SY5Y cells (FtMt group) after OGD/R insult. Overlay images of cells labelled with both MitoSOX Red and Mito Tracker Green indicate that OGD/R treatment led to significant increases in mitochondrial ROS levels relative to the control group (Con) in the WT and Vector cells, while FtMt overexpression reversed the OGD/R-induced mitochondrial ROS accumulation (Fig. 4A–B). Meanwhile, FtMt overexpression also alleviated OGD/R-mediated MDA generation in the cells (Fig. 4C). However, the GSH content, a key intracellular antioxidant, in FtMt overexpressing cells was much higher than that in wild type cells after OGD/R treatment, indicating FtMt increased the antioxidative capacity of neuronal cells (Fig. 4D). Considering the effects of FtMt on cellular iron distribution and regulation, we conjecture that the mitochondrial free iron can, at least in part, affect the generation of mitochondrial ROS. We next detected the expression of mitoferrin1 (Mfrn1), a mitochondrial iron importer, and the mitochondrial ferrous iron content in cells after OGD/R insult. OGD/R injury increased the expression of Mfrn1 as well as the free iron levels in mitochondria. FtMt overexpression reversed this increase (Supplementary Figs. 3A–D). These results confirm that FtMt exhibits robust

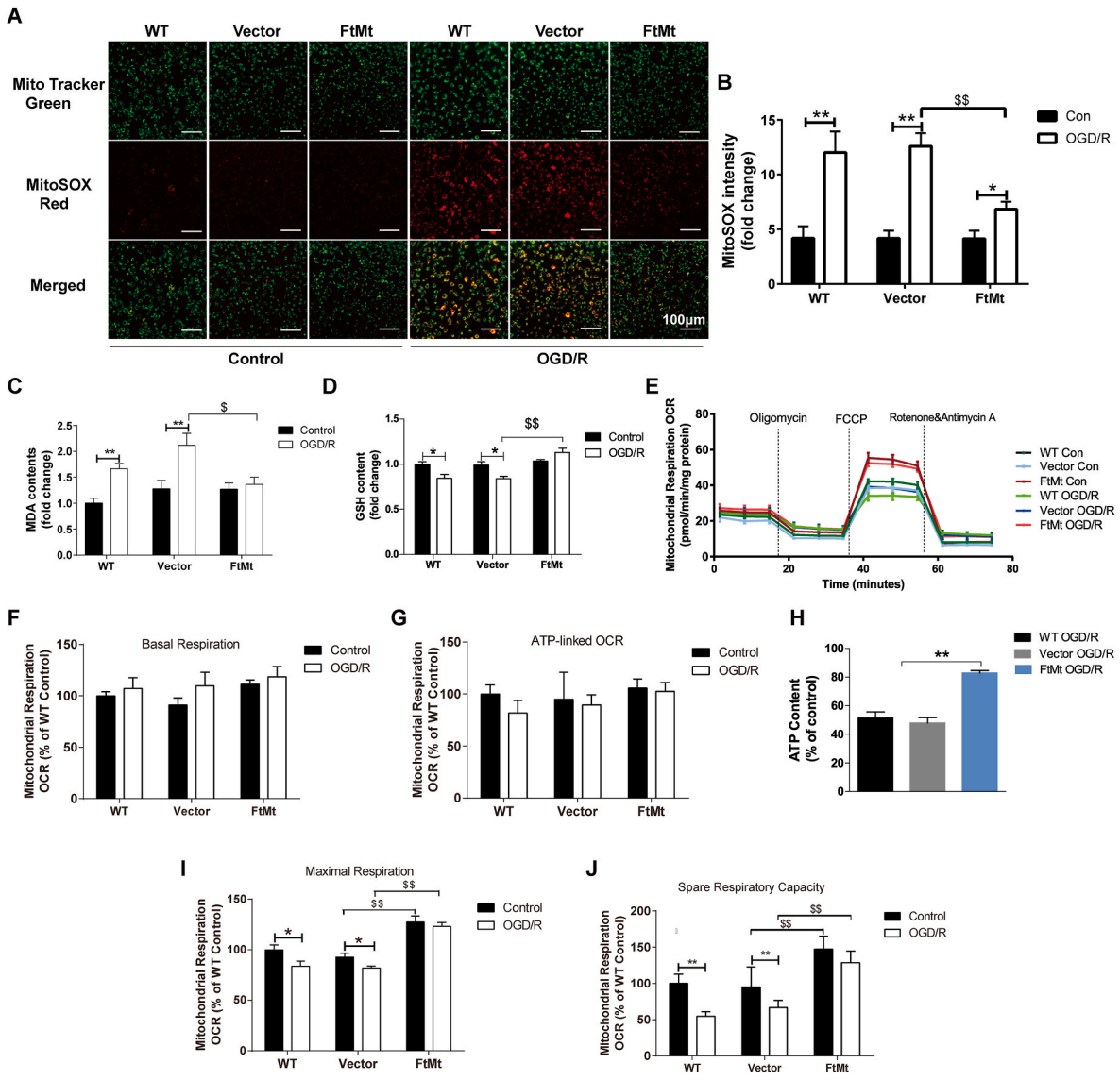

Fig. 4. FtMt overexpression restricts ROS generation and enhances mitochondrial bioenergetics during OGD/R injury. (A) Representative images showing co-localization of MitoSOX Red fluorescence and Mito Tracker Green fluorescence in SH-SY5Y cells (WT), stable FtMt-overexpressing SH-SY5Y cells (FtMt) and pcDNA3.1 (−) empty vector-transfected cells (Vector) after OGD/R treatment. (B) Quantitative evaluation of MitoSOX fluorescence intensity (n = 3). (C) MDA and (D) GSH contents, as quantified using commercially available assays (n = 3). The oxygen consumption rate (OCR) of the Con and OGD/R groups, as determined using a Seahorse XF analyzer. (E) OCR was recorded at baseline and after the sequential injection of oligomycin (2 μM), FCCP (8 μM) and a mixture of rotenone and antimycin A (1 μM) (n = 4). (F) Basal respiration, (G) ATP -linked OCR, (H) quantitative results of the levels of ATP (I) maximal respiration, and (J) spare respiratory capacity. The results are presented as the mean ± SEM. $^{*/\$}P < 0.05$, $^{**/\$\$}P < 0.01$. (For interpretation of the references to colour in this figure legend, the reader is referred to the Web version of this article.)

antioxidative capacity against I/R-induced oxidative stress.

Next, we explored the effect of FtMt overexpression on OGD/R-induced mitochondrial dysfunction. WT, Vector, and FtMt cells were subjected to OGD/R insult and OCR values were assessed using a Seahorse XFp Analyzer (Fig. 4E). We did not observe any distinguishable differences in basal respiration or ATP-linked respiration in either group after OGD (5 h) followed by 18 h of reperfusion. This is likely due to differences between culture plate and the whole animal (Fig. 4F–G). However, the ATP contents in the WT OGD/R and Vector OGD/R groups were decreased to nearly 50% of the control group; FtMt overexpression attenuated this OGD/R-induced ATP depletion (Fig. 4H). The maximal respiration and spare respiratory capacity were significantly diminished in WT and Vector cells after OGD/R insult compared with the control. These decreases were markedly reversed by FtMt overexpression (Fig. 4I–J). Significant increases in maximal respiration and spare respiratory capacity were also observed in cells under normal conditions, which confirms the capability of FtMt to enhance mitochondrial bioenergetics. We additionally measured the effects of FtMt on OGD/R-induced MMP dissipation by JC-1. As shown in Supplementary Figs. 4A–B, the control group cells exhibited mainly red fluorescence, while OGD/R-injured cells showed significantly enhanced green fluorescence, indicating that OGD/R caused MMP dissipation. However, the red/green ratio in the FtMt-overexpressing cells was higher than that in the WT and Vector groups after OGD/R insult, indicating that FtMt alleviated the OGD/R-induced MMP decrease. Taken together, these results confirm the key role of FtMt in maintaining mitochondrial bioenergetics and function.

3.5. *Overexpression of FtMt enhances glucose metabolism in neuronal cells after OGD/R injury*

Glucose is the major oxidative substrate for energy generation in the

brain. Mitochondrial impairment can serve as a signal of energy changes and thus modulate glucose metabolism [42]. To examine the role of FtMt in glucose metabolism, we recorded ECAR under OGD/R conditions (Fig. 5A). Our data indicated that the basal ECAR was increased in all experimental groups under OGD/R relative to the control, with the increase more apparent in the FtMt overexpressing OGD/R group (Fig. 5B). The maximal ECAR and glycolysis reserve capacity in the WT OGD/R and Vector OGD/R groups were similar with their respective control groups. Intriguingly, greater glucose consumption and increased glycolysis reserve capacity were observed in FtMt overexpressing cells after OGD/R insult (Fig. 5C–D). Notably, marked increases in the basal ECAR, maximal ECAR and glycolysis reserve capacity were observed in the FtMt overexpressing SH-SY5Y cells also under normal conditions, indicating the important role of FtMt in promoting glucose metabolism. These results reveal that FtMt overexpression significantly promotes glucose metabolism in neuronal cells, and the cell metabolism was comprehensively ameliorated in FtMt overexpressing cells under OGD/R conditions.

3.6. Overexpression of FtMt enhances the pentose-phosphate pathway in neuronal cells after OGD/R injury

The pentose-phosphate pathway (PPP) is a major branch of glucose metabolism, which is known to be essential for antioxidant protection [43]. To explore whether FtMt affects the activation of the PPP during OGD/R injury, we measured NADPH content and G6PDH activity, key biomarkers of PPP, in neuronal cells after OGD/R insult. The NADPH content was significantly decreased in the three experimental groups under OGR/R conditions compared with the control group, indicating reduced energy metabolism and increased oxidative damage in cells after OGD/R treatment. Again, FtMt overexpression alleviated the decline (Fig. 6A). The NADPH content in the FtMt OGD/R group was higher than that in the WT OGD/R and Vector OGD/R groups, which also consistent with the high level of GSH in FtMt OGD/R group. Meanwhile, OGD/R injury increased the activity of G6PDH compared with the control, revealing an enhancement in the activation of the PPP under OGD/R conditions. The overexpression of FtMt facilitated the increase in G6PDH activity, compared with the control groups, under OGD/R injury (Fig. 6B). These results suggest that FtMt enhances the activation of the PPP of glucose metabolism in OGD/R-injured neuronal cells. This function helps to strengthen the antioxidant defences and maintain the redox balance during OGD/R damage.

4. Discussion

The antioxidant role of FtMt in neurodegenerative diseases by chelating free iron has been reported in our previous studies [28,44]. In the current study, we demonstrated that FtMt exerts antioxidant effects in I/R injury by enhancing mitochondrial bioenergetics and regulating glucose metabolism via the pentose-phosphate pathway, thus preventing mitochondrial ROS generation and strengthening the antioxidant defenses of neuronal cells. As a result, FtMt alleviates mitochondria-dependent apoptosis and ER stress (ATF4/ATF6-CHOP pathway)-associated apoptosis in I/R, thus attenuating I/R-induced brain damage and neurological deficits (Fig. 7).

Mitochondria, as the powerhouse of the cell, play a central role in energy metabolism through oxidative phosphorylation, therefore maintaining mitochondrial function is important for neuronal function and survival, especially under I/R conditions [45]. However, due to the presence of the electron transport chain, mitochondria have been recognized as the major source of ROS. Up to 2% of the oxygen in the mitochondria undergoes one-electron reduction to generate superoxide anion radicals and hydrogen peroxide when passing through the electron transport chain [46]. The hydrogen peroxide can then be converted to hydroxyl radicals with the participation of ferrous iron in the Fenton reaction [47]. Following ischemia reperfusion injury, the reduction of blood supply and calcium overload result in mitochondrial dysfunction [48]. Imbalanced mitochondrial electron transport during reperfusion

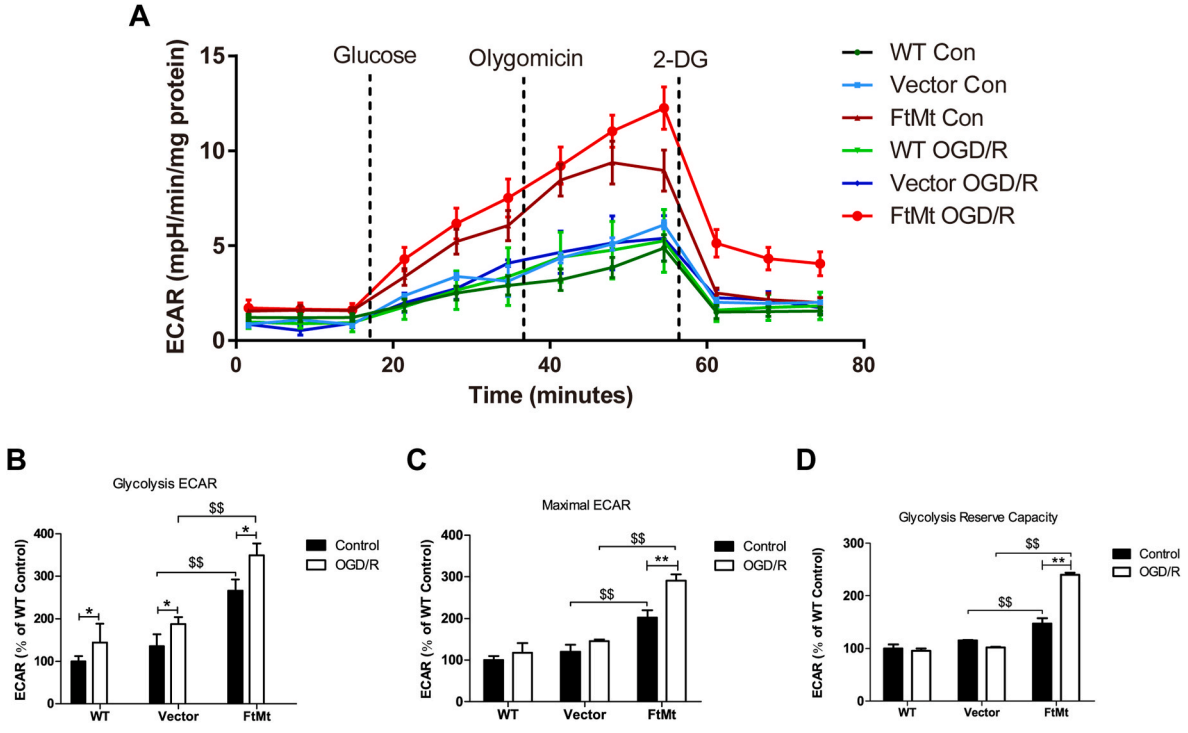

Fig. 5. Overexpression of FtMt enhances glucose metabolism in neuronal cells under OGD/R insult. SH-SY5Y (WT) cells, empty vector transfectants (Vector) and FtMt-overexpressing transfectants (FtMt) were subjected to OGD/R insult. Next, the ECAR of the Con and OGD/R groups was assessed with a Seahorse XF analyzer. (A) ECAR was recorded after the sequential injection of glucose (10 mM), oligomycin (2 μM), and 2-deoxy-glucose (50 mM). (B) Basal ECAR, (C) maximal ECAR and (D) the reserve capacity were calculated. The results are presented as the mean ± SEM, n = 4, $^{*}P < 0.05$, $^{**/\$\$}P < 0.01$.

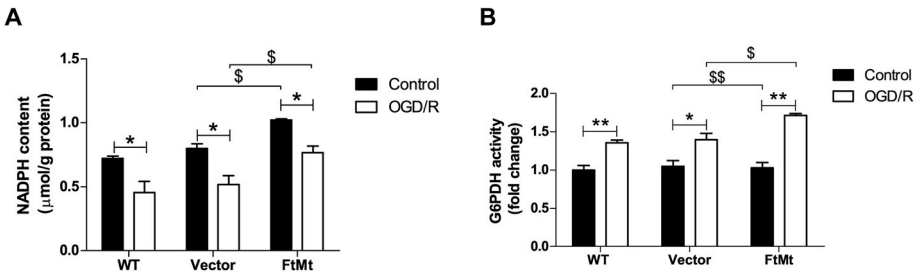

Fig. 6. Overexpression of FtMt enhances the pentose-phosphate pathway in neuronal cells under OGD/R insult. SH-SY5Y cells (WT), empty vector transfectants (vector) and FtMt-overexpressing transfectants (FtMt) were subjected to OGD/R insult. (A) NADPH content and (B) G6DPH activity were quantified using a commercially available assay. The results are presented as the mean ± SEM, n = 4, $^{*/\$}P < 0.05$, $^{**/\$\$}P < 0.01$.

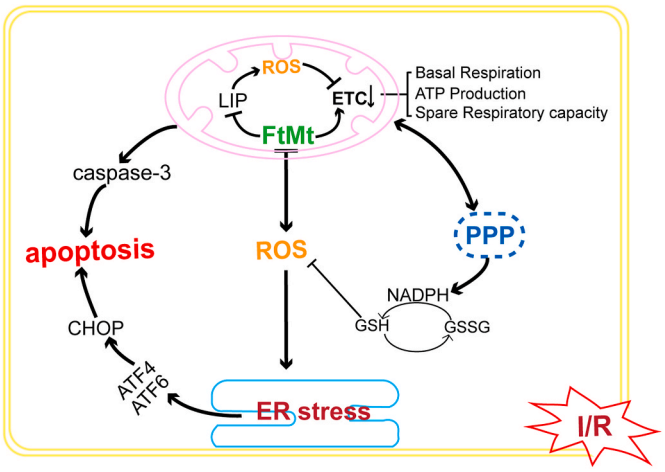

Fig. 7. Schematic representation of the proposed antioxidative mechanism of FtMt in cerebral I/R. Ischemic stroke causes mitochondrial dysfunction and ROS overproduction, resulting in mitochondria dependent apoptosis and ER stress-associated apoptosis in the brain. FtMt reduces cerebral I/R-induced oxidative stress by maintaining mitochondrial bioenergetics and regulating glucose metabolism via the pentose-phosphate pathway, thus inhibiting ROS overproduction, and preventing neuronal deficits in I/R.

leads to increased ROS production, ultimately leading to neuronal apoptosis [49]. In addition, overproduction of ROS causes damage to lipids and proteins, which further impairs mitochondrial function and leads to a decrease in the MMP [50]. Therefore, mitochondria are both the source and target of ROS in I/R injury. I/R-induced mitochondrial dysfunction facilitates the generation of ROS, while the intracellular ROS leads to more severe mitochondrial damage. In the current study, we found that I/R led to marked oxidative stress and mitochondrial dysfunction, including impaired mitochondrial respiration and decreased MMP. These effects were significantly suppressed by the presence of FtMt, which enhanced mitochondrial bioenergetics and inhibited ROS overproduction (Fig. 3; Fig. 4).

Glucose is the major metabolic substrate for energy production. As a high energy consuming organ, the brain, unlike most other tissues, relies almost completely on glucose for energy generation [43]. Aberrant glucose metabolism has been identified as a pivotal pathological mechanism of ischemic stroke [51]. Once delivered into the cell, glucose will be phosphorylated to glucose-6-phophate (G6P) by hexokinase. The G6P can be further metabolized by glycolysis or the pentose-phosphate pathway to produce pyruvate, which is fully oxidized in the tricarboxylic acid cycle to synthesize ATP under normoxic conditions, or converted to lactate under hypoxic conditions [52]. In this study, we found that OGD/R injury facilitated glucose metabolism in SH-SY5Y cells, with basal ECAR upregulated in the OGD/R group (Fig. 5B). FtMt overexpression induced greater glucose consumption, indicating that FtMt protects neurons from energy stress under OGD/R condition by enhancing glucose metabolism (Fig. 5). Previous studies have indicated that glycolysis is less active in neurons, due to the low levels of the glycolysis regulating enzyme, 6-phosphofructo-2-kinase/fructose-2, 6-bisphosphatase isoform 3 (PFKFB3), and the glycolysis activator, fructose 2,6-bisphosphate [53]. Neurons preferentially utilize G6D through PPP under oxidative stress [54]. PPP can produce nicotinamide adenine dinucleotide phosphate (NADPH), which is required for the reduction of glutathione disulfide (GSSG) to glutathione (GSH) to remove excess ROS [54]. At the same time, we indeed observed that the GSH content in FtMt overexpressing cell was higher than in wild type cell under OGD/R conditions (Fig. 4D). Therefore, we further explored whether FtMt affects glucose metabolism via PPP. Our results revealed that the activity of G6PDH, the rate-limiting enzyme of PPP, was increased after OGD/R stimulation, indicating the activation of PPP was enhanced in OGD/R-injured neurons. FtMt overexpression enhanced the G6PDH activity and, as a result, facilitated the production of NADPH (Fig. 6). Our results provide the first evidence that FtMt promotes glucose metabolism via PPP to strengthen the antioxidant capacity in the I/R injury.

Taken together, our data reveal that FtMt plays an important antioxidative role in cerebral I/R injury. On the one hand, FtMt alleviated I/R-induced mitochondrial dysfunction, thus preserving the energy demand in neurons and preventing mitochondria dependent ROS production. On the other hand, FtMt facilitated the generation of NADPH by PPP, thus accelerating the scavenging of ROS in cells after I/R injury. In addition, we also observed that FtMt attenuated OGD/R-induced ferrous iron accumulation in mitochondria (Supplementary Figs. 3C–D), which may suppress ROS production through the Fenton reaction, as previously reported. Studies have shown that iron is crucial for mitochondria to maintain respiratory activity and membrane potential [55]. We propose that FtMt may participate in mitochondrial respiration by regulating iron traffic in mitochondria, but more in-depth studies are needed to explore the precise mechanism by which FtMt enhances mitochondrial bioenergetics. Interestingly, previous study indicated that the activation of PPP is increased in brain of a conditional mouse with decreased mitochondrial ROS [56]. Iron overload reduces the expression and activity of G6PDH in liver and spleen of mice with high iron diet [57,58]. These evidences suggest that the iron content and mitochondrial redox state are regulators or key factors that affecting the activation of PPP in cell. Therefore, we suppose that FtMt overexpression reduces mitochondrial ROS generation and suppresses mitochondrial and cytosolic iron accumulation in cerebral I/R, thus stimulating glucose metabolism via PPP. Further studies are needed to verify the role of FtMt in glucose metabolism in neuronal cells after I/R.

Rigorous research has shown that I/R-induced ROS overproduction can act directly on the mitochondria and initiate classical mitochondria-dependent apoptosis, which includes a decreased Bcl2/Bax ratio and caspase 3 activation. In recent years, ER stress-associated apoptosis has also been implicated in the pathogenesis of ischemic stroke. Inhibiting ER stress with compounds can significantly protect neurons against

ischemic injury [59]. Accumulation of ROS, calcium dysregulation and inflammation in the I/R brain can initiate the unfolded protein response, leading to ER stress [15]. Our previous studies revealed a protective role of FtMt in restricting mitochondria-dependent apoptosis in neurodegenerative diseases [60]. However, the relevance of FtMt to the ER stress pathway under stress conditions has not been reported. Our results demonstrate that the ATF4-CHOP pathway and ATF6 pathway were significantly activated after I/R injury (Fig. 1E–I). An increase in CHOP levels is critical in ER stress to initiate apoptosis through down-regulation of Bcl2 and up-regulation of ROS [13]. The ablation of FtMt significantly aggravated the activation of ER stress response (Fig. 1E–I), as well as the activation of the mitochondrial apoptosis pathway (Fig. 1B–D), which led to an increased proportion of apoptotic cells in the brain after I/R (Fig. 1A). Consistently, FtMt overexpression attenuated OGD/R-induced apoptosis and neuronal damage (Fig. 2A). Therefore, our data indicate that FtMt can restrict ER stress-induced apoptosis in cerebral I/R by inhibiting ROS accumulation.

5. Conclusion

In the present study, we demonstrated that FtMt reduces cerebral I/R-induced oxidative stress by maintaining mitochondrial bioenergetics and regulating glucose metabolism via the pentose-phosphate pathway, thus inhibiting ER stress-associated apoptosis, and preventing neuronal deficits in I/R.

Author contributions statement

Yan-Zhong Chang and Peina Wang designed the research. Peina Wang performed most of the experiments with the help of Yashuo Zhao, Yuanyuan Liu and Yanmei Cui. Huiyuan Bai and Zhongda Li conducted part of the *in vitro* experiments. Peina Wang, Yashuo Zhao, Yuanyuan Liu and Huiyuan Bai analyzed the data. Peina Wang wrote the manuscript with help from Yan-Zhong Chang.

Declaration of competing interest

The authors declare no conflicts of interest.

Acknowledgements

The work was supported by the National Natural Science Foundation of China (grant numbers 31520103908) and the Key Project of Natural Science Foundation of Hebei Province, China (E2021205003).

Appendix A. Supplementary data

Supplementary data to this article can be found online at https://doi.org/10.1016/j.redox.2022.102475.

References

[1] B.C.V. Campbell, D.A. De Silva, M.R. Macleod, S.B. Coutts, L.H. Schwamm, S. M. Davis, G.A. Donnan, Ischaemic stroke, Nat. Rev. Dis. Prim. 5 (2019) 70, https://doi.org/10.1038/s41572-019-0118-8.
[2] J.M. Wardlaw, V. Murray, E. Berge, G.J. del Zoppo, Thrombolysis for acute ischaemic stroke, Cochrane Database Syst. Rev. 2014 (2014), https://doi.org/10.1002/14651858.CD000213.pub3.
[3] K. Jackman, A. Kunz, C. Iadecola, Modeling focal cerebral ischemia in vivo, Methods Mol. Biol. 793 (2011) 195–209, https://doi.org/10.1007/978-1-61779-328-8_13.
[4] J. Bai, P.D. Lyden, Revisiting cerebral postischemic reperfusion injury: new insights in understanding reperfusion failure, hemorrhage, and edema, Int. J. Stroke 10 (2015) 143–152, https://doi.org/10.1111/ijs.12434.
[5] Y.P. Zhang, Y. Zhang, Z. Bin Xiao, Y.B. Zhang, J. Zhang, Z.Q. Li, Y. Bin Zhu, CFTR prevents neuronal apoptosis following cerebral ischemia reperfusion via regulating mitochondrial oxidative stress, J Mol Med 96 (2018) 611–620, https://doi.org/10.1007/s00109-018-1649-2.
[6] M.D. Brand, Mitochondrial generation of superoxide and hydrogen peroxide as the source of mitochondrial redox signaling, Free Radic. Biol. Med. 100 (2016) 14–31, https://doi.org/10.1016/j.freeradbiomed.2016.04.001.
[7] A. Boveris, B. Chance, The mitochondrial generation of hydrogen peroxide. General properties and effect of hyperbaric oxygen, Biochem. J. 134 (1973) 707–716, https://doi.org/10.1042/bj1340707.
[8] S. Sun, F. Hu, J. Wu, S. Zhang, Cannabidiol attenuates OGD/R-induced damage by enhancing mitochondrial bioenergetics and modulating glucose metabolism via pentose-phosphate pathway in hippocampal neurons, Redox Biol. 11 (2017) 577–585, https://doi.org/10.1016/j.redox.2016.12.029.
[9] Z. He, N. Ning, Q. Zhou, S.E. Khoshnam, M. Farzaneh, Mitochondria as a therapeutic target for ischemic stroke, Free Radic. Biol. Med. 146 (2020) 45–58, https://doi.org/10.1016/j.freeradbiomed.2019.11.005.
[10] R.C.S. Seet, C.-Y.J. Lee, B.P.L. Chan, V.K. Sharma, H.-L. Teoh, N. Venketasubramanian, E.C.H. Lim, W.-L. Chong, W.-F. Looi, S.-H. Huang, B.K. C. Ong, B. Halliwell, Oxidative damage in ischemic stroke revealed using multiple biomarkers, Stroke 42 (2011) 2326–2329, https://doi.org/10.1161/STROKEAHA.111.618835.
[11] S.S. Andrabi, S. Parvez, H. Tabassum, Progesterone induces neuroprotection following reperfusion-promoted mitochondrial dysfunction after focal cerebral ischemia in rats, Dis Model Mech 10 (2017) 787–796, https://doi.org/10.1242/dmm.025692.
[12] Y. Lai, P. Lin, M. Chen, Y. Zhang, J. Chen, M. Zheng, J. Liu, H. Du, R. Chen, X. Pan, N. Liu, H. Chen, Restoration of L-OPA1 alleviates acute ischemic stroke injury in rats via inhibiting neuronal apoptosis and preserving mitochondrial function, Redox Biol. 34 (2020), 101503, https://doi.org/10.1016/j.redox.2020.101503.
[13] Q. Xin, B. Ji, B. Cheng, C. Wang, H. Liu, X. Chen, J. Chen, B. Bai, Endoplasmic reticulum stress in cerebral ischemia, Neurochem. Int. 68 (2014) 18–27, https://doi.org/10.1016/j.neuint.2014.02.001.
[14] Y.F. Dong, L.X. Wang, X. Huang, W.J. Cao, M. Lu, J.H. Ding, X.L. Sun, G. Hu, Kir6.1 knockdown aggravates cerebral ischemia/reperfusion-induced neural injury in mice, CNS Neurosci. Ther. 19 (2013) 617–624, https://doi.org/10.1111/cns.12117.
[15] L. Gong, Y. Tang, R. An, M. Lin, L. Chen, J. Du, RTN1-C mediates cerebral ischemia/reperfusion injury via ER stress and mitochondria-associated apoptosis pathways, Cell Death Dis. 8 (2017), e3080, https://doi.org/10.1038/cddis.2017.465.
[16] J. Drysdale, P. Arosio, R. Invernizzi, M. Cazzola, A. Volz, B. Corsi, G. Biasiotto, S. Levi, Mitochondrial ferritin: a new player in iron metabolism, Blood Cells Mol. Dis. 29 (2002) 376–383, https://doi.org/10.1006/bcmd.2002.0577.
[17] P. Santambrogio, G. Biasiotto, F. Sanvito, S. Olivieri, P. Arosio, S. Levi, Mitochondrial ferritin expression in adult mouse tissues, J. Histochem. Cytochem. 55 (2007) 1129–1137, https://doi.org/10.1369/jhc.7A7273.2007.
[18] P. Arosio, S. Levi, Cytosolic and mitochondrial ferritins in the regulation of cellular iron homeostasis and oxidative damage, Biochim. Biophys. Acta Gen. Subj. 1800 (2010) 783–792, https://doi.org/10.1016/j.bbagen.2010.02.005.
[19] Z.H. Shi, G. Nie, X.L. Duan, T. Rouault, W.S. Wu, B. Ning, N. Zhang, Y.Z. Chang, B. L. Zhao, Neuroprotective mechanism of mitochondrial ferritin on 6-hydroxydopamine- induced dopaminergic cell damage: implication for neuroprotection in Parkinson's disease, Antioxidants Redox Signal. 13 (2010) 783–796, https://doi.org/10.1089/ars.2009.3018.
[20] W.S. Wu, Y.S. Zhao, Z.H. Shi, S.Y. Chang, G.J. Nie, X.L. Duan, S.M. Zhao, Q. Wu, Z. L. Yang, B.L. Zhao, Y.Z. Chang, Mitochondrial ferritin attenuates β-amyloid-induced neurotoxicity: reduction in oxidative damage through the Erk/P38 mitogen-activated protein kinase pathways, Antioxidants Redox Signal. 18 (2013) 158–169, https://doi.org/10.1089/ars.2011.4285.
[21] H. Guan, H. Yang, M. Yang, D. Yanagisawa, J.P. Bellier, M. Mori, S. Takahata, T. Nonaka, S. Zhao, I. Tooyama, Mitochondrial ferritin protects SH-SY5Y cells against H2O2-induced oxidative stress and modulates α-synuclein expression, Exp. Neurol. 291 (2017) 51–61, https://doi.org/10.1016/j.expneurol.2017.02.001.
[22] G. Gao, N. Zhang, Y.Q. Wang, Q. Wu, P. Yu, Z.H. Shi, X.L. Duan, B.L. Zhao, W. S. Wu, Y.Z. Chang, Mitochondrial ferritin protects hydrogen peroxide-induced neuronal cell damage, Aging Dis 8 (2017) 458–470, https://doi.org/10.14336/AD.2016.1108.
[23] A. Campanella, G. Isaya, H.A. O'Neill, P. Santambrogio, A. Cozzi, P. Arosio, S. Levi, The expression of human mitochondrial ferritin rescues respiratory function in frataxin-deficient yeast, Hum. Mol. Genet. 13 (2004) 2279–2288, https://doi.org/10.1093/hmg/ddh232.
[24] P. Wang, Y. Cui, Q. Ren, B. Yan, Y. Zhao, P. Yu, G. Gao, H. Shi, Mitochondrial ferritin attenuates cerebral ischaemia/reperfusion injury by inhibiting ferroptosis, Cell Death Dis. (2021), https://doi.org/10.1038/s41419-021-03725-5.
[25] T.B. Bartnikas, D.R. Campagna, B. Antiochos, H. Mulhern, C. Pondarré, M. D. Fleming, Characterization of mitochondrial ferritin-deficient mice, Am. J. Hematol. 85 (2010) 958–960, https://doi.org/10.1002/ajh.21872.
[26] E.S. Connolly, C.J. Winfree, D.M. Stern, R.A. Solomon, D.J. Pinsky, Procedural and strain-related variables significantly affect outcome in a murine model of focal cerebral ischemia, Neurosurgery 38 (1996).
[27] L.D. McCullough, F. Liu, Middle cerebral artery occlusion model in rodents: methods and potential pitfalls, J. Biomed. Biotechnol. 2011 (2011), https://doi.org/10.1155/2011/464701.
[28] Z.H. Shi, G. Nie, X.L. Duan, T. Rouault, W.S. Wu, B. Ning, N. Zhang, Y.Z. Chang, B. L. Zhao, Neuroprotective mechanism of mitochondrial ferritin on 6-hydroxydopamine- induced dopaminergic cell damage: implication for neuroprotection in Parkinson's disease, Antioxidants Redox Signal. 13 (2010) 783–796, https://doi.org/10.1089/ars.2009.3018.

[29] Y. Huang, J. Wang, J. Cai, Y. Qiu, H. Zheng, X. Lai, X. Sui, Y. Wang, Q. Lu, Y. Zhang, M. Yuan, J. Gong, W. Cai, X. Liu, Y. Shan, Z. Deng, Y. Shi, Y. Shu, L. Zhang, W. Qiu, L. Peng, J. Ren, Z. Lu, A.P. Xiang, Targeted homing of CCR2-overexpressing mesenchymal stromal cells to ischemic brain enhances post-stroke recovery partially through PRDX4-mediated blood-brain barrier preservation, Theranostics 8 (2018) 5929–5944, https://doi.org/10.7150/thno.28029.

[30] P. Wang, Q. Wu, W. Wu, H. Li, Y. Guo, P. Yu, G. Gao, Z. Shi, B. Zhao, Y.Z. Chang, Mitochondrial ferritin deletion exacerbates β -Amyloid-Induced neurotoxicity in mice, Oxid. Med. Cell. Longev. 2017 (2017), 1020357, https://doi.org/10.1155/2017/1020357.

[31] J.J. Wen, C.B. Cummins, R.S. Radhakrishnan, Burn-induced cardiac mitochondrial dysfunction via interruption of the PDE5A-cGMP-PKG pathway, Int. J. Mol. Sci. 21 (2020) 1–15, https://doi.org/10.3390/ijms21072350.

[32] A. Alessandrini, S. Namura, M.A. Moskowitz, J. v Bonventre, MEK1 protein kinase inhibition protects against damage resulting from focal cerebral ischemia, Proc. Natl. Acad. Sci. U. S. A. 96 (22) (1999) 12866–12869, https://doi.org/10.1073/pnas.96.22.12866.

[33] S. Namura, K. Iihara, S. Takami, I. Nagata, H. Kikuchi, K. Matsushita, M. A. Moskowitz, J. v Bonventre, A. Alessandrini, Intravenous administration of MEK inhibitor U0126 affords brain protection against forebrain ischemia and focal cerebral ischemia, Proc. Natl. Acad. Sci. U. S. A. 98 (20) (2001) 11569–11574, https://doi.org/10.1073/pnas.181213498.

[34] M. Bi, A. Gladbach, J. van Eersel, A. Ittner, M. Przybyla, A. van Hummel, S. W. Chua, J. van der Hoven, W.S. Lee, J. Müller, J. Parmar, G. von Jonquieres, H. Stefen, E. Guccione, T. Fath, G.D. Housley, M. Klugmann, Y.D. Ke, L.M. Ittner, Tau exacerbates excitotoxic brain damage in an animal model of stroke, Nat. Commun. 8 (2017), https://doi.org/10.1038/s41467-017-00618-0.

[35] H. Zhou, W. shuang Yang, Y. Li, T. Ren, L. Peng, H. Guo, J. feng Liu, Y. Zhou, Y. Zhao, L. chao Yang, X. Jin, Oleoylethanolamide attenuates apoptosis by inhibiting the TLR4/NF-κB and ERK1/2 signaling pathways in mice with acute ischemic stroke, Naunyn-Schmiedeberg's Arch. Pharmacol. 390 (2017) 77–84, https://doi.org/10.1007/s00210-016-1309-4.

[36] L. Zhan, D. Li, D. Liang, B. Wu, P. Zhu, Y. Wang, W. Sun, E. Xu, Activation of Akt/FoxO and inactivation of MEK/ERK pathways contribute to induction of neuroprotection against transient global cerebral ischemia by delayed hypoxic postconditioning in adult rats, Neuropharmacology 63 (2012) 873–882, https://doi.org/10.1016/j.neuropharm.2012.06.035.

[37] T. Peng, S. Li, L. Liu, C. Yang, M. Farhan, L. Chen, Q. Su, W. Zheng, Artemisinin attenuated ischemic stroke induced cell apoptosis through activation of ERK1/2/CREB/BCL-2 signaling pathway in vitro and in vivo, Int. J. Biol. Sci. 18 (2022) 4578–4594, https://doi.org/10.7150/ijbs.69892.

[38] T.C.H. Tan, D.H.G. Crawford, L.A. Jaskowski, V.N. Subramaniam, A.D. Clouston, D. I. Crane, K.R. Bridle, G.J. Anderson, L.M. Fletcher, Excess iron modulates endoplasmic reticulum stress-associated pathways in a mouse model of alcohol and high-fat diet-induced liver injury, Lab. Invest. 93 (2013) 1295–1312, https://doi.org/10.1038/labinvest.2013.121.

[39] S.A. Andrabi, H.C. Kang, J.F. Haince, Y. il Lee, J. Zhang, Z. Chi, A.B. West, R. C. Koehler, G.G. Poirier, T.M. Dawson, V.L. Dawson, Iduna protects the brain from glutamate excitotoxicity and stroke by interfering with poly(ADP-ribose) polymer-induced cell death, Nat Med 17 (2011) 692–699, https://doi.org/10.1038/nm.2387.

[40] W. Tu, X. Xu, L. Peng, X. Zhong, W. Zhang, M.M. Soundarapandian, C. Balel, M. Wang, N. Jia, W. Zhang, F. Lew, S.L. Chan, Y. Chen, Y. Lu, DAPK1 interaction with NMDA receptor NR2B subunits mediates brain damage in stroke, Cell 140 (2010) 222–234, https://doi.org/10.1016/j.cell.2009.12.055.

[41] X. Zhang, H. Yan, Y. Yuan, J. Gao, Z. Shen, Y. Cheng, Y. Shen, R.R. Wang, X. Wang, W.W. Hu, G. Wang, Z. Chen, Cerebral ischemia-reperfusion-induced autophagy protects against neuronal injury by mitochondrial clearance, Autophagy 9 (2013) 1321–1333, https://doi.org/10.4161/auto.25132.

[42] A. Almeida, P. Cidad, M. Delgado-Esteban, E. Fernández, P. García-Nogales, J. P. Bolaños, Inhibition of mitochondrial respiration by nitric oxide: its role in glucose metabolism and neuroprotection, J. Neurosci. Res. 79 (2005) 166–171, https://doi.org/10.1002/jnr.20281.

[43] G.A. Dienel, Brain glucose metabolism: integration of energetics with function, Physiol. Rev. 99 (2019) 949–1045, https://doi.org/10.1152/physrev.00062.2017.

[44] W.S. Wu, Y.S. Zhao, Z.H. Shi, S.Y. Chang, G.J. Nie, X.L. Duan, S.M. Zhao, Q. Wu, Z. L. Yang, B.L. Zhao, Y.Z. Chang, Mitochondrial ferritin attenuates β-amyloid-induced neurotoxicity: reduction in oxidative damage through the Erk/P38 mitogen-activated protein kinase pathways, Antioxidants Redox Signal. 18 (2013) 158–169, https://doi.org/10.1089/ars.2011.4285.

[45] E.I. Rugarli, T. Langer, Mitochondrial quality control: a matter of life and death for neurons, EMBO J. 31 (2012) 1336–1349, https://doi.org/10.1038/emboj.2012.38.

[46] A. Boveris, B. Chance, The mitochondrial generation of hydrogen peroxide. General properties and effect of hyperbaric oxygen, Biochem. J. 134 (1973) 707–716, https://doi.org/10.1042/bj1340707.

[47] T. Carbonell, R. Rama, Iron, oxidative stress and early neurological deterioration in ischemic stroke, Curr. Med. Chem. 14 (2007) 857–874, https://doi.org/10.2174/092986707780363014.

[48] P. Bakthavachalam, P.S.T. Shanmugam, Mitochondrial dysfunction – silent killer in cerebral ischemia, J. Neurol. Sci. 375 (2017) 417–423, https://doi.org/10.1016/j.jns.2017.02.043.

[49] J. min Liang, H. yang Xu, X. jie Zhang, X. Li, H. bo Zhang, P. fei Ge, Role of mitochondrial function in the protective effects of ischaemic postconditioning on ischaemia/reperfusion cerebral damage, J. Int. Med. Res. 41 (2013) 618–627, https://doi.org/10.1177/0300060513476587.

[50] N.P. Visavadiya, M.L. McEwen, J.D. Pandya, P.G. Sullivan, B.J. Gwag, J. E. Springer, Antioxidant properties of Neu2000 on mitochondrial free radicals and oxidative damage, Toxicol. Vitro 27 (2013) 788–797, https://doi.org/10.1016/j.tiv.2012.12.011.

[51] J. Geng, Y. Zhang, S. Li, S. Li, J. Wang, H. Wang, J. Aa, G. Wang, Metabolomic profiling reveals that reprogramming of cerebral glucose metabolism is involved in ischemic preconditioning-induced neuroprotection in a rodent model of ischemic stroke, J. Proteome Res. 18 (2019) 57–68, https://doi.org/10.1021/acs.jproteome.8b00339.

[52] T. Kristián, Metabolic stages, mitochondria and calcium in hypoxic/ischemic brain damage, Cell Calcium 36 (2004) 221–233, https://doi.org/10.1016/j.ceca.2004.02.016.

[53] I. Juaristi, L. Contreras, P. González-Sánchez, I. Pérez-Liébana, L. González-Moreno, B. Pardo, A. del Arco, J. Satrústegui, The response to stimulation in neurons and astrocytes, Neurochem. Res. 44 (2019) 2385–2391, https://doi.org/10.1007/s11064-019-02803-7.

[54] L. Cao, D. Zhang, J. Chen, Y.Y. Qin, R. Sheng, X. Feng, Z. Chen, Y. Ding, M. Li, Z. H. Qin, G6PD plays a neuroprotective role in brain ischemia through promoting pentose phosphate pathway, Free Radic. Biol. Med. 112 (2017) 433–444, https://doi.org/10.1016/j.freeradbiomed.2017.08.011.

[55] M. Fujimaki, N. Furuya, S. Saiki, T. Amo, Y. Imamichi, N. Hattori, Iron supply via NCOA4-mediated ferritin degradation maintains mitochondrial functions, Mol. Cell Biol. 39 (2019) 1–13, https://doi.org/10.1128/mcb.00010-19.

[56] C. Vicente-Gutierrez, N. Bonora, V. Bobo-Jimenez, D. Jimenez-Blasco, I. Lopez-Fabuel, E. Fernandez, C. Josephine, G. Bonvento, J.A. Enriquez, A. Almeida, J. P. Bolaños, Astrocytic mitochondrial ROS modulate brain metabolism and mouse behaviour, Nat Metab 1 (2019) 201–211, https://doi.org/10.1038/s42255-018-0031-6.

[57] H. Budak, H. Ceylan, E.F. Kocpinar, N. Gonul, O. Erdogan, Expression of glucose-6-phosphate dehydrogenase and 6-phosphogluconate dehydrogenase in oxidative stress induced by long-term iron toxicity in rat liver, J. Biochem. Mol. Toxicol. 28 (2014) 217–223, https://doi.org/10.1002/jbt.21556.

[58] N. Gonul Baltaci, C. Guler, H. Ceylan, S.N. Kalin, S. Adem, E.F. Kocpinar, O. Erdogan, H. Budak, In vitro and in vivo effects of iron on the expression and activity of glucose 6-phosphate dehydrogenase, 6-phosphogluconate dehydrogenase, and glutathione reductase in rat spleen, J. Biochem. Mol. Toxicol. 33 (2019) 1–7, https://doi.org/10.1002/jbt.22229.

[59] K. Srinivasan, S.S. Sharma, Edaravone offers neuroprotection in a diabetic stroke model via inhibition of endoplasmic reticulum stress, Basic Clin. Pharmacol. Toxicol. 110 (2012) 133–140, https://doi.org/10.1111/j.1742-7843.2011.00763.x.

[60] G. Gao, Y.Z. Chang, Mitochondrial ferritin in the regulation of brain iron homeostasis and neurodegenerative diseases, Front. Pharmacol. 5 (FEB) (2014) 1–7, https://doi.org/10.3389/fphar.2014.00019.